Am J Cancer Res 2021;11(1):236-250
www.ajcr.us /ISSN:2156-6976/ajcr0126041

Original Article

Nuclear translocation of the receptor tyrosine kinase c-MET reduces the treatment efficacies of olaparib and gemcitabine in pancreatic ductal adenocarcinoma cells

Yuan Gao[1,2], Mei-Kuang Chen[2], Yu-Yi Chu[2], Liuqing Yang[2], Dihua Yu[2], Yingbin Liu[1], Mien-Chie Hung[3,2,4]

[1]Department of Biliary-Pancreatic Surgery, Renji Hospital, School of Medicine, Shanghai Jiao Tong University, Shanghai 200127, China; [2]Department of Molecular and Cellular Oncology, The University of Texas MD Anderson Cancer Center, Houston 77030, TX, USA; [3]Graduate Institute of Biomedical Sciences, Research Center for Cancer Biology, Center for Molecular Medicine, China Medical University, Taichung 404, Taiwan; [4]Department of Biotechnology, Asia University, Taichung 413, Taiwan

Received November 10, 2020; Accepted November 21, 2020; Epub January 1, 2021; Published January 15, 2021

Abstract: Pancreatic ductal adenocarcinoma (PDAC) is an aggressive cancer that lack effective therapeutic strategies. The response rate of PDAC for treatment with gemcitabine, a current first-line chemotherapeutic for this tumor, is lower than 20%. Identifying key targetable molecules that mediate gemcitabine resistance and developing novel strategies for precision PDAC medicine are urgently needed. Most PDACs have either intratumoral hypoxia or high reactive oxygen species (ROS) production; cytotoxic chemotherapy can elevate ROS production in PDACs. Although excessive ROS production leads to oxidative damage of macromolecules such as DNA, pancreatic cancer cells can survive high DNA damage stress levels. Therefore, identifying molecular mechanisms of overcoming ROS-induced stress in pancreatic cancer cells is important for developing novel therapeutic strategies. ROS-induced DNA damage is predominantly repaired via poly (ADP-ribose) polymerase 1 (PARP1)-mediated DNA repair mechanisms. A recent clinical trial reported that PARP inhibitors are effective in treating pancreatic patients carrying BRCA mutations. However, only less than 10% of pancreatic cancer patients bearing BRCA mutated tumors. Activation of the receptor tyrosine kinase c-MET positively correlates with poor prognosis for PDAC, and our previous study showed that nuclear c-MET can phosphorylate PARP1 at tyrosine 907 under ROS stimulation to promote DNA repair. As described herein, we proposed to expand PARP inhibitor-targeted therapy to more pancreatic cancer patients regardless of BRCA mutation status by combining olaparib, a PARP inhibitor, with c-MET inhibitors as we demonstrated in our previous studies in breast cancer. In this prospective study, we found that ROS-inducing chemotherapeutic drugs such as gemcitabine and doxorubicin stimulated nuclear accumulation of c-MET in BxPC-3 and L3.6pl pancreatic cancer cells. We further showed that combining a c-MET inhibitor with gemcitabine or a PARP inhibitor induced more DNA damage than monotherapy did. Moreover, we demonstrated the synergistic antitumor effects of c-MET inhibitors combined with a PARP inhibitor or gemcitabine in eliminating pancreatic cancer cells. These data suggested that accumulation of ROS in pancreatic cancer cells promotes nuclear localization of c-MET, resulting in resistance to both chemotherapy and PARP inhibitors. Our findings suggest that combining c-MET inhibitors with PARP inhibitors or gemcitabine is a novel, rational therapeutic strategy for advanced pancreatic cancer.

Keywords: Pancreatic ductal adenocarcinoma, resistance, chemotherapy, targeted therapy, precision medicine, reactive oxygen species, PARP inhibitor, tivantinib, DNA damage

Introduction

Pancreatic cancer has become the fourth leading cause of death in the United States, and it is also one of the most aggressive and lethal cancers worldwide [1, 2]. The 5-year relative survival rate is 9%, which is the lowest among all types of cancer [2]. As a characteristic of pancreatic ductal adenocarcinoma (PDAC) in particular, destruction of adjacent structures leads to the pain and reduced quality of life [3]. Surgical resection is the only strategy that can potentially cure PDAC, and adjuvant chemotherapy has increased survival rates for pancreatic cancer patients [1]. However, for patients who are ineligible for surgical interventions due to

locally advanced or metastatic PDAC, chemotherapy and targeted therapy are by far the best options to extend survival. Unfortunately, treatment with gemcitabine, a first-line chemotherapeutic agent, was effective in less than 20% of pancreatic cancer patients [4]. Furthermore, resistance of PDAC to chemotherapy is a major challenge. In pancreatic cancer patients, small-molecule inhibitors targeting tyrosine kinases, such as tivantinib, cabozantinib, and crizotinib, are currently under clinical trial investigations [5, 6]. However, in a phase 2 trial, treatment with cabozantinib failed to benefit patients with PDAC [7, 8]. While most targeted therapies for PDAC are currently in phase 1 clinical trials, identifying effective therapeutic strategies for advanced PDAC is urgently needed.

PDAC is composed with dense stroma that occupied 60-90% of the volume of tumor [9]. In the tumor environment generated by its complicated stromal compartments, PDAC commonly has intratumoral hypoxia and high reactive oxygen species (ROS) production [10]. Although ROS induce oxidation of macromolecules such as DNA, proteins, and lipids, pancreatic cancer cells can survive ROS-induced stress at relatively high but tolerable levels. Recent evidence suggests that NADPH oxidase-mediated production of ROS plays a pivotal role in the development of gemcitabine resistance [12, 13]. Therefore, understanding the molecular mechanisms used by PDAC to overcome ROS-induced cellular stress is important. An inhibitor of poly(ADP-ribose) polymerase 1 (PARP1), a key protein in repairing ROS-induced DNA damage [14], is one of the targeted therapeutic agents that can stimulate accumulation of ROS and ROS-induced DNA damage [15-17]. A recent clinical trial showed that treatment with a PARP inhibitor benefited patients with advanced pancreatic cancer and germline *breast cancer susceptibility protein* (BRCA) mutations [18]. At the end of 2019, the U.S. Food and Drug Administration approved olaparib for patients with deleterious germline BRCA-mutated metastatic PDAC as a maintenance treatment. However, less than 10% of PDAC patients carry BRCA mutations [19]. Therefore, our goal is to extend PARP inhibitor-based therapy to PDAC patients regardless of BRCA mutation status by combining a PARP inhibitor with other targeted therapeutic agents.

Among the targeted therapeutic agents under investigation in PDAC clinical trials, we chose c-MET inhibitors as our first priority in developing a combination treatment with a PARP inhibitor. In our previous studies, we demonstrated that c-MET translocates from the cell membrane into the nucleus in response to ROS in breast cancers [20], and we further showed that c-MET phosphorylates PARP1 at the tyrosine 907 (Tyr907) residue, resulting in PARP inhibitor resistance in breast, ovarian, and liver cancer cells [21-24]. However, the stimuli for nuclear c-MET localization may vary by cancer type [25]. The correlations among high oxidative microenvironment, c-MET nuclear translocation and therapeutic resistance in PDAC is unknown. Therefore, there is a need to characterize the function of nuclear c-MET in PDAC for developing effective therapeutic strategies. In the present study, we first demonstrated that ROS-inducing chemotherapeutic drugs like gemcitabine and doxorubicin promote nuclear accumulation of c-MET in PDAC cell lines, which may partially explain their resistance to chemotherapy. Using H_2O_2 as the source of ROS, we showed that treatment with H_2O_2 induced nuclear c-MET translocation in a dose- and time-dependent manner in PDAC cell lines. We further showed that c-MET interacted with PARP1 in the nucleus and that PARP1 phosphorylation at Tyr907 was partially inhibited by treatment with tivantinib, a selective c-MET inhibitor. Moreover, combinations of c-MET inhibitors with a PARP inhibitor enhanced DNA damage and had a synergistic effect in eliminating pancreatic cancer cells. Our data suggested that ROS-induced cellular stress promotes nuclear localization of c-MET, which results in the resistance of pancreatic cancer cells to chemotherapy as well as PARP inhibitor-based therapy. As described herein, we proposed combining c-MET inhibitors with a PARP inhibitor or gemcitabine as a new therapeutic strategy for advanced pancreatic cancer.

Materials and methods

Antibodies and reagents

The antibodies used in this study were those against c-MET (C-12, sc-10; Santa Cruz Biotechnology, Santa Cruz, CA), lamin B1 (12987-1-AP; Proteintech, Rosemont, IL), calregulin (sc-11398; Santa Cruz Biotechnology), α-tubulin

(T5168; Sigma-Aldrich, St. Louis, MO), phosphorylated nuclear factor (NF)-κB (Ser536, #3036S; Cell Signaling Technology, Danvers, MA), nuclear factor-κB (#4764; Cell Signaling Technology), phosphorylated Akt (Ser473, #3787; Cell Signaling Technology), Akt (#9272S; Cell Signaling Technology), phosphorylated p44/42 mitogen-activated protein kinase (Thr202/Tyr204, #4370T; Cell Signaling Technology), p44/42 (Erk1/2, #4695T; Cell Signaling Technology), hypoxia-inducible factor-1α (NBP2-75978SS; Novus Biologicals, Littleton, CO), GAPDH (sc-32233; Santa Cruz Biotechnology), PARP (11040-RP01; Sino Biological, Wayne, PA, and 9532S; Cell Signaling Technology), phosphorylated γH2AX (Ser139, #9718P; Cell Signaling Technology), phosphorylated BRCA1 (Ser1524, #9009P; Cell Signaling Technology), phosphorylated Chk1 (Ser345, #2348P; Cell Signaling Technology), phosphorylated p53 (Ser15, #9286P; Cell Signaling Technology), p53 (sc-56182; Santa Cruz Biotechnology), and phosphorylated tyrosine (4G10, #05-321; MilliporeSigma, Burlington, MA). A murine anti-phosphorylated Tyr907-PARP1 antibody was generated as described previously [21].

Gemcitabine (G-4199), crizotinib (C-7900), and olaparib (O-9201) were purchased from LC Laboratories (Woburn, MA); tivantinib (#17135) was obtained from Cayman Chemical (Ann Arbor, MI); and H_2O_2 (#216763) was purchased form Sigma-Aldrich. VECTASHIELD PLUS Antifade Mounting Medium with DAPI (H-2000) was purchased from Vector Laboratories (Burlingame, CA).

Cell culture

The human PDAC cell lines BxPC-3 and L3.6pl were obtained from the ATCC (Manassas, VA) and maintained in Dulbecco's modified Eagle's medium/Nutrient Mixture F-12 supplemented with 10% fetal bovine serum at 37°C in a humidified incubator with a 5% CO_2 atmosphere. The cell lines were validated via short tandem repeat DNA fingerprinting at The University of Texas MD Anderson Cancer Center, and the cells were negative for mycoplasma infection.

Cell fractionation

Nuclear and non-nuclear cell fractionations were conducted as described previously [20]. Briefly, PDAC cells were harvested at 80-90% confluence and lysed in Nori lysis buffer (20 mM HEPES, pH 7.0, 10 mM KCl, 0.5% NP-40, 2 mM $MgCl_2$, 2 mM Na_3VO_4, 1 mM PMSF, 0.15 mg/ml aprotinin) on ice for at least 10 min. Next, cells were homogenized using a tight Dounce tissue grinder. After cell lysates were centrifuged at 1500×*g* for 5 min, the supernatants were collected as non-nuclear cell fractions. Nuclei pellet were further washed with the lysis buffer before solubilized in NTEN buffer (150 mM NaCl, 1 mM EDTA, 20 mM Tris-HCl, pH 8.0, 0.5% NP-40, protease inhibitor mixture). Finally, cell extracts were centrifuged at maximum speed for at least 10 min. The supernatant was collected as a nuclear fraction.

Western blot analysis

Cell lysates and immunoprecipitants were separated on 8% sodium dodecyl sulfate-polyacrylamide gel electrophoresis gels and transferred onto 0.22-μm polyvinylidene fluoride membranes. The membranes were blocked and incubated with primary antibodies at 4°C overnight, which was followed by horseradish peroxidase-conjugated secondary antibody hybridization. The signals were detected using Clarity Max ECL Western Blotting substrates (Bio-Rad, Hercules, CA). Images of the membrane were quantified using the Image Studio Lite software program (version 5.2; LI-COR, Lincoln, NE). Tubulin or GAPDH was used as a loading control.

To detect proteins in cell fractionation samples. 25-40 μg of total proteins were loaded in each lane of a gel for sodium dodecyl sulfate-polyacrylamide gel electrophoresis. The same amounts of nuclear and non-nuclear fraction protein fractions were used in Western blot analysis. The nuclear envelope protein lamin B was used to indicate the cell nuclear fraction. Calregulin was used to indicate the presence of endoplasmic reticulum proteins.

Immunofluorescence and confocal microscopy

BxPC-3 and L3.6pl cells were seeded on chamber slides (Labtek, Scotts Valley, CA) for at least 18 h before the treatments indicated in each experiment. After treatment, the cells were fixed with 4% paraformaldehyde, permeabilized with 0.2% Triton X-100/PBS, blocked with 5% goat serum/PBS with Tween 20, and stained with the indicated primary or fluorescence-

labeled secondary antibodies. Primary antibodies were diluted in 3% goat serum/PBS with Tween 20 at the following ratios: anti-c-MET antibody, 1:100; anti-PARP1 antibody, 1:100; and anti-phosphorylated γH2AX (Ser139) antibody, 1:200. DNA was counterstained with a DAPI-containing mounting solution before cells were examined and imaged under a Zeiss LSM 710 laser microscope (White Plains, NY). Results of florescent signals were processed and analyzed using ZEN software (version 2.3; Zeiss) and ImageJ software (Fiji, 1.53c; National Institutes of Health, Bethesda, MD).

Immunoprecipitation

The BxPC-3 cells were pre-incubated with or without 1 μM tivantinib for 4 h before being stimulated with 5 mM H_2O_2 for 25 min prior to lysate collection. In brief, cells were lysed in NETN buffer (150 mM NaCl, 1 mM EDTA, 20 mM Tris-HCl, pH 8.0, 0.5% NP-40, 1% PMSF, protease inhibitor cocktail), and 500 μg of total protein per sample was used for immunoprecipitation, whereas 100 μg of total protein was collected as the input. Cell lysates were incubated with 1 μg of a primary antibody or anti-IgG antibody at 4°C overnight and then incubated with SureBeads Protein G Magnetic Beads (Bio-Rad) for 2 h. Next, the beads were washed three times with PBS with Tween 20. Precipitants were eluted from the magnetic beads using a sodium dodecyl sulfate-polyacrylamide gel electrophoresis sample buffer and subjected to Western blotting.

Cell viability assay

BxPC-3 (1,800 cells/well) and L3.6pl (2,400 cells/well) cells were seeded in a 96-well plate and cultured overnight before treatments were administered. Culture media containing drugs or inhibitors were refreshed on the third day of treatment. After treatment for 96 h, cells were incubated for 2 h with 0.5 mg/ml thiazolyl blue tetrazolium bromide (Sigma-Aldrich), and formazan crystals were dissolved in dimethyl sulfoxide. The optical density at 590 nm was measured, and survival percentages were calculated by normalizing the optical density value for each treatment group according to that for the control group. Combination index (CI) experiments were designed as suggested by Chou [26]. Results were analyzed using CompuSyn software (CompuSyn, Paramus, NJ). All experiments were performed in triplicate.

Colony formation assay

BxPC-3 (1,500 cells/well) and L3.6pl (1,800 cells/well) cells were seeded into a 12-well plate 18 h before the treatments, as indicated. Inhibitor-containing media were refreshed every 3 days. After treatment for 10-14 days, cells were fixed using 4% paraformaldehyde. Cell colonies were stained with 0.5% crystal violet before being quantified. The colony formation rate was calculated by normalizing the number of colonies in each well according to those in the vehicle-treated well in each group. All experiments were performed in triplicate.

Statistical analysis

Signal intensities in Western blots images were analyzed using Image Studio Lite (version 5.2). Signals for c-MET were normalized according to those for loading control proteins such as lamin B and calregulin in each sample before being normalized to the signals of those in the control groups. Results were quantified individually for each independent repeated experiment. Fold changes in Western blot signals were analyzed using a nonparametric Friedman test with the Prism 8.0 software program (GraphPad Software, San Diego, CA). The co-localization coefficients for c-MET in nuclei were analyzed and processed using ZEN software (version 2.1). The different co-localization coefficients were compared using an unpaired nonparametric Mann-Whitney test with Prism 8.0. The γH2AX foci per nucleus were analyzed and counted using ImageJ (Fiji, 1.53c). The γH2AX focus counts were compared using a nonparametric Kruskal-Wallis test with Prism 8.0. *P* values less than 0.05 were considered significant.

Results

Chemotherapeutic drugs promote nuclear c-MET translocation in pancreatic cancer cells

Although we reported that treatment with ROS-producing agents such as H_2O_2 and doxorubicin can induce nuclear c-MET translocation in breast cancer cells [20], whether gemcitabine can induce a similar phenomenon in pancreatic cancer cells is unknown. Therefore, we first investigated whether nuclear c-MET accumulation positively correlates with ROS generation. We stimulated BxPC-3 and L3.6pl PDAC cells with multiple concentrations of H_2O_2, and we

found that the accumulation of nuclear c-MET occurred in an H_2O_2 dose-dependent manner and that exposure to 1 mM H_2O_2 induced significant nuclear c-MET transport (**Figure 1A**). Time-course experiments demonstrated that 15-min H_2O_2 stimulation was sufficient for inducing nuclear c-MET accumulation in both BxPC-3 and L3.6pl cells (**Figure 1B**). To count the BxPC-3 and L3.6pl cells containing nuclear c-MET, we performed immunofluorescent staining of them. Immunostaining for c-MET in the control group demonstrated that it was mainly located outside the nuclei under normal culture conditions (**Figure 1C**). c-MET then aggregated in the perinuclear region and nuclei in response to H_2O_2 stimulation. Quantitative analyses showed more BxPC-3 and L3.6pl cells containing nuclear c-MET after H_2O_2 stimulation than under normal culture conditions (**Figure 1C**). Taken together, these results demonstrated that c-MET can efficiently translocate into the nucleus under H_2O_2 stimulation in a dose- and time-dependent manner.

To determine whether nuclear c-MET translocation can be stimulated by chemotherapy, we treated BxPC-3 and L3.6pl cells with three clinical first-line chemotherapeutic agents: gemcitabine, cisplatin, and doxorubicin. We observed that accumulation of nuclear c-MET in both cell lines varied in response to treatment with the three drugs (**Figure 2A**). Particularly, we found significant accumulation of c-MET in the nucleus after gemcitabine- and doxorubicin-based treatment. However, cisplatin-induced nuclear c-MET accumulation was not markedly different from that in vehicle-treated cells. We further confirmed the activation of ROS-responding pathways in these PDAC cells using treatment with H_2O_2 as a positive control. Expression of representative molecules in response to ROS, such as Ser-536-phosphorylated nuclear factor-κB, Ser473-phosphorylated Akt, and Thr202- and Tyr204-phosphorylated Erk, was much higher after treatment with gemcitabine and doxorubicin than after the vehicle in both BxPC-3 and L3.6pl cells (**Figure 2B**), demonstrating activation of ROS-induced cellular response. In summary, treatment with gemcitabine and doxorubicin activated the ROS pathway and promoted nuclear c-MET translocation in pancreatic cancer cells.

Inhibition of c-MET activity sensitizes PDAC cells to treatment with gemcitabine

Because exposure to gemcitabine promotes nuclear c-MET accumulation and nuclear localized receptor tyrosine kinases are known to regulate cellular responses to stress [25], we asked whether inhibition of c-MET activity can sensitize PDAC cells to treatment with gemcitabine. To that end, we chose two c-MET inhibitors used clinically: tivantinib, which is a specific inhibitor of c-MET activity, and crizotinib, which can inhibit the activity of multiple kinases, including c-MET [27, 28]. We treated BxPC-3 and L3.6pl cells with gemcitabine and crizotinib or tivantinib and then examined the synergistic effects of these two combinations using the CI. In brief, a CI below 1 indicates synergistic effects of drugs [26]. In the BxPC-3 and L3.6pl cells, both combinations had good synergistic effects (CI < 0.5) in killing most of the tumor cells (fraction affected (Fa) > 0.8) (**Figure 3A**). Also, whereas both combinations had similar synergistic effects in BxPC-3 cells, the combination of crizotinib and gemcitabine had a greater synergistic effect than the combination of tivantinib and gemcitabine did in L3.6pl cells.

Using γH2AX foci as indicators of DNA breakage, we found that although gemcitabine and tivantinib can induce DNA breaks by themselves, the combination of these two agents induced formation of more γH2AX foci than the single-agent treatments did (**Figure 3B**). Moreover, we found that the combination treatment significantly activated the molecules involved in DNA damage response, including Ser15-phosphorylated p53, Ser15-24-phosphorylated BRCA1, and Ser345-phosphorylated Chk1 (**Figure 3C**). These results showed that severe DNA damage occurred in both BxPC-3 and L3.6pl cells when treated with the combination of tivantinib and gemcitabine. Taken together, these data demonstrated synergy between gemcitabine exposure and c-MET inhibition.

Nuclear c-MET interacts with PARP1 and phosphorylates PARP1 in response to ROS in PDAC cells

On the basis of the findings described above, we asked the question of why inhibition of c-MET activity can increase the sensitivity of PDAC cells to treatment with gemcitabine

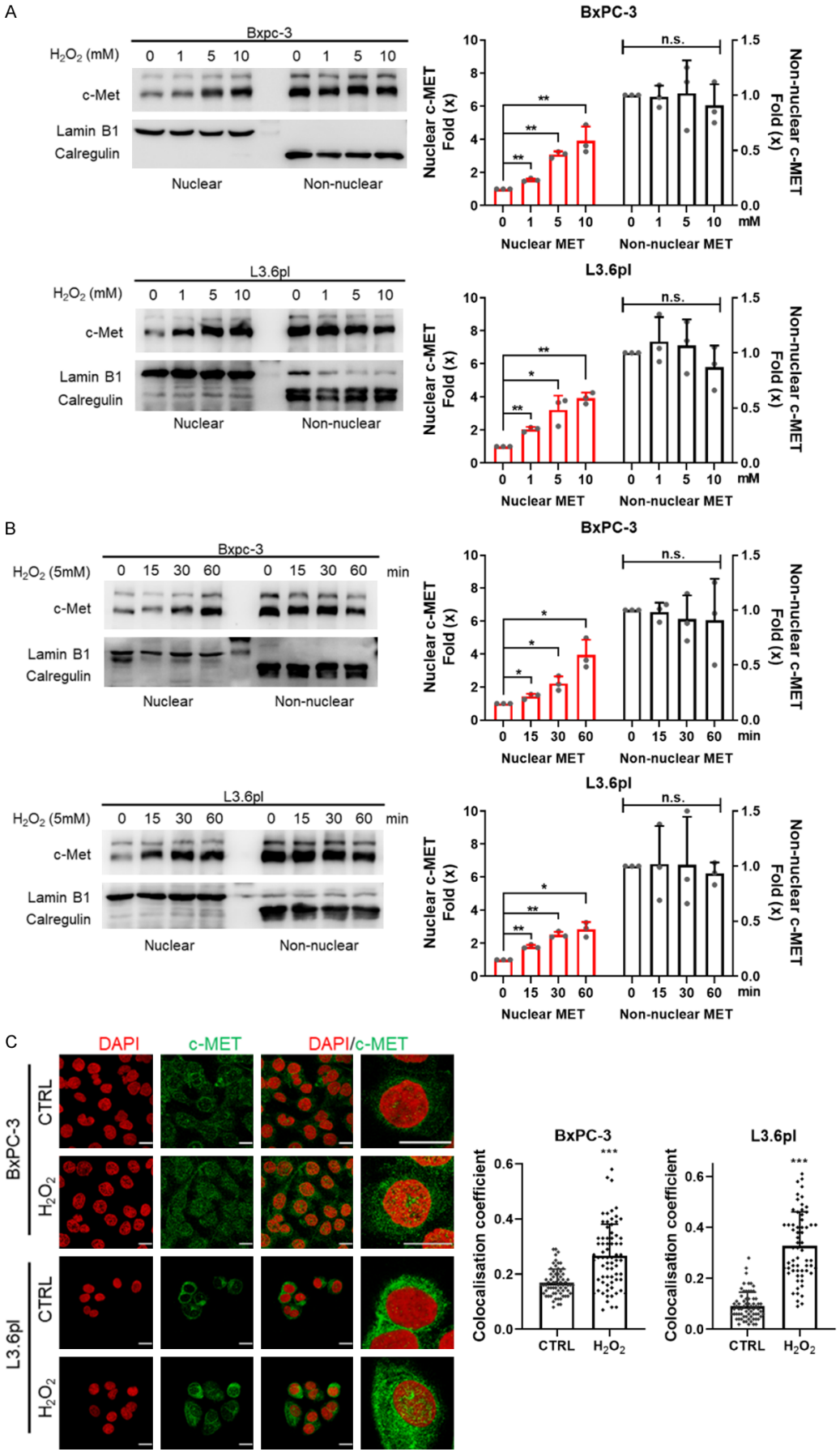
A
Bxpc-3
H2O2 (mM)
0 1 5 10 0 1 5 10
c-Met
Lamin B1
Calregulin
Nuclear
Non-nuclear
BxPC-3
Nuclear c-MET Fold (x)
Non-nuclear c-MET Fold (x)
n.s.
Nuclear MET
Non-nuclear MET
mM
L3.6pl
B
Bxpc-3
H2O2 (5mM)
0 15 30 60 0 15 30 60 min
BxPC-3
L3.6pl
C
DAPI
c-MET
DAPI/c-MET
BxPC-3
L3.6pl
CTRL
H2O2
Colocalisation coefficient
***

Figure 1. Chemotherapeutic drugs and H_2O_2 can induce c-MET nuclear accumulation in pancreatic cancer cell lines. A. BxPC-3 and L3.6pl cells were treated with increasing concentrations of H_2O_2 for 30 min and subjected to cellular fractionation. Both nuclear and non-nuclear cell fractions were examined by Western blotting with the indicated antibodies. Fold changes in three independent experiments are shown in the histograms as mean (± standard deviation [S.D.]) values. *P < 0.05; **P < 0.01. n.s., not significant. B. BxPC-3 and L3.6pl cells were incubated with 5 mM H_2O_2 for duration of times as indicated before being harvested for Western blotting. Fold changes in three independent experiments are shown in the histograms as mean (± S.D.) values. *P < 0.05; **P < 0.01. n.s., not significant. C. BxPC-3 and L3.6pl cells were treated with 5 mM H_2O_2 for 30 min before immunostaining with an anti-c-MET antibody (green fluorescence) and DAPI (pseudocolored red). Images of anti-c-MET antibody- and DAPI-stained cells were merged to show the nuclear locations of c-MET (yellow). Insets, enlarged views of nuclear c-MET localization. Scale bars, 20 μm. Z-stack images with a 0.25-μm interval between each slice are shownin sequence to demonstrate that c-MET localized into the nucleus under H_2O_2 stimulation. Scale bars, 20 μm. Statistical analyses were performed using the co-localization coefficients for nuclear c-MET and DAPI. Each nucleus is represented by a dot (n > 60). Quantification results are shown as mean (± S.D.) values. ***P < 0.001.

through induction of excessive DNA damage. Our previous experience with breast cancer showed that although c-MET mostly acts as a membrane receptor kinase, it plays important roles in DNA damage repair [21-24]. We speculated that, as in breast cancer cells, c-MET can interact with PARP1 in pancreatic cell lines. To confirm this, we conducted an immunoprecipitation assay to examine the interaction between c-MET and PARP1. As expected, c-MET interacted with PARP1 in both BxPC-3 and L3.6pl cells, and PARP1 precipitation with c-MET increased in response to ROS exposure (**Figure 4A** and **4B**, left panel). We further found that the interaction between PARP1 and c-MET can be partially interrupted by pretreating cells with tivantinib. We also observed ROS-induced co-localization of c-MET and PARP1 in nuclei under a confocal microscope (**Figure 4C**).

Because c-MET is a well-known tyrosine kinase, we examined the tyrosine phosphorylation of PARP1 in PDAC cells using antibodies against pan-tyrosine phosphorylation (clone 4G10) and Tyr907-phosphorylated PARP1. Substantially lower pan-tyrosine and Tyr907 phosphorylation was observed in cells treated with tivantinib and H_2O_2 than in cells treated with H_2O_2 alone (**Figure 4A** and **4B**, right panel). This indicated that Tyr907 is one of the PARP1 tyrosine sites phosphorylated by c-MET in PDAC cells. Taken together, these data suggested that in PDAC cells, c-MET translocated into the nucleus, where c-MET interacted with and phosphorylated PARP1 in response to exposure to H_2O_2.

Combined inhibition of c-MET and PARP1 activity has a synergistic antitumor effect

Because c-MET interacted with PARP1 in pancreatic cancer cells, we then asked if a combination treatment with c-MET and PARP inhibitors can have a synergistic antitumor effect. We examined the CIs for the c-MET inhibitors crizotinib and tivantinib combined with a PARP inhibitor (olaparib). Both combinations exhibited synergy (CI < 1) in BxPC-3 and L3.6pl cells (**Figure 5A**). We further performed a colony formation assay to validate the synergy observed in these CI experiments. Consistent with the CI measurement, the combination of tivantinib and olaparib suppressed the clonogenicity of the PDAC cells more than either agent did alone in both BxPC-3 and L3.6pl cells (**Figure 5B**).

Moreover, we examined DNA damage and the activation of DNA repair pathways in response to treatment with the combination of tivantinib and olaparib in PDAC cells. We found more γH2AX foci per nucleus in BxPC-3 cells treated with this combination than in cells treated with either agent alone, demonstrating that the combination of tivantinib and olaparib induced excessive DNA damage in these cells (**Figure 5C**). Also, elevated levels of Ser15-phosphorylated p53, Ser1524-phosphorylated BRCA1, and Ser345-phosphorylated Chk1 indicated activation of DNA damage responses in both BxPC-3 and L3.6pl cells after simultaneous treatment with tivantinib and olaparib (**Figure 5D**). Thus, simultaneous inhibition of c-MET and PARP activity can be an effective approach to improve the treatment of PDAC.

Discussion

Increasing evidence suggests that treatment with gemcitabine induces ROS production in pancreatic cancer cells and thus leads to metabolic reprogramming and promotes stem-like characteristics in cancer cells [12, 29]. This phenomenon may compromise the efficacy of and induce resistance to chemotherapy for pancreatic cancer [29]. Therefore, we focused

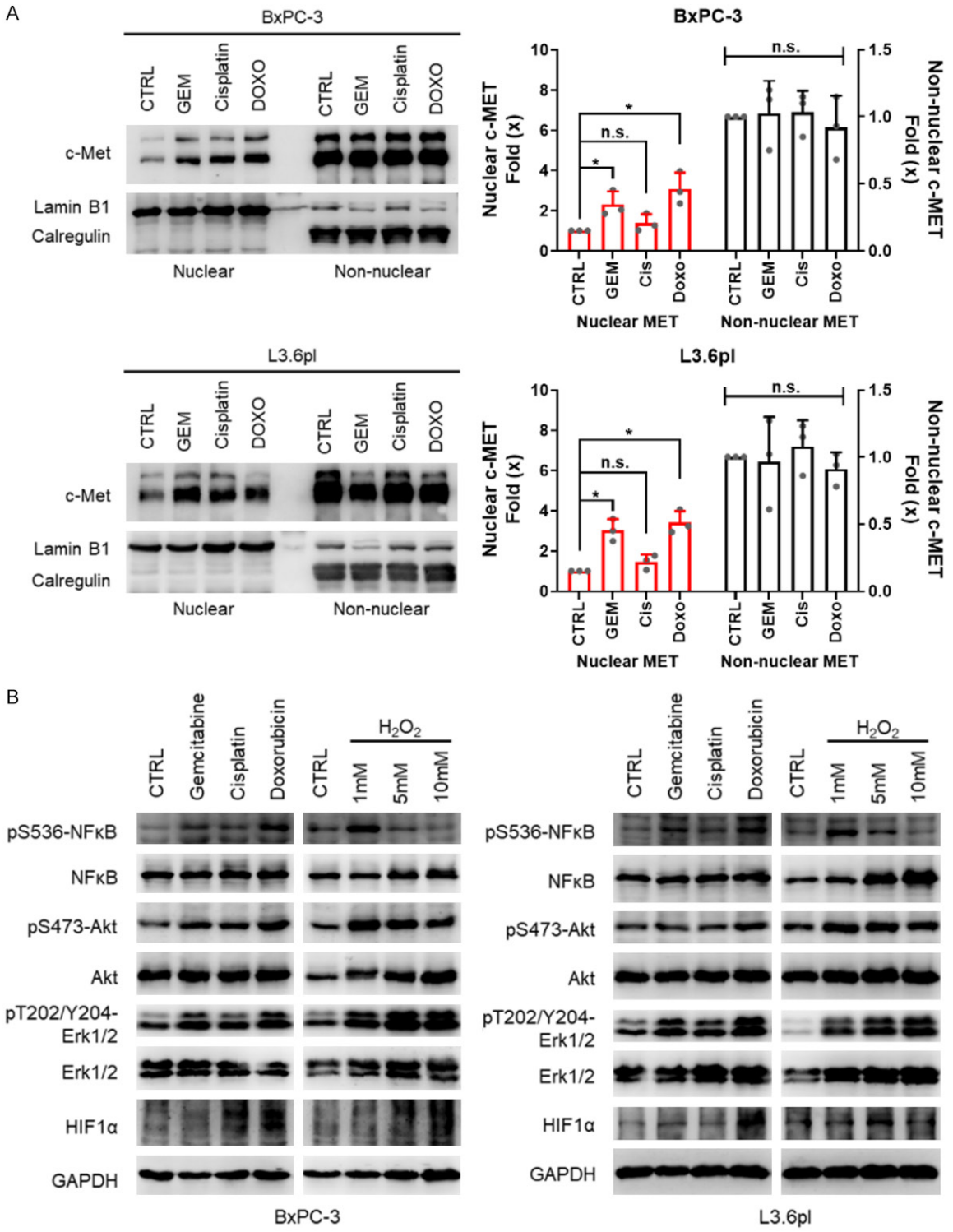

Figure 2. A. BxPC-3 and L3.6pl cells were treated with gemcitabine (BxPC-3, 200 nM; L3.6pl, 120 nM), cisplatin (BxPC-3, 2.5 μM; L3.6pl, 2 μM), or doxorubicin (BxPC-3, 600 nM; L3.6pl, 400 nM) for 8 h and subjected to cellular fractionation followed by Western blotting with the indicated antibodies. The nuclear envelope protein lamin B and endoplasmic reticulum protein calregulin were used to indicate nuclear and nonnuclear fractions, respectively. Anti-lamin B and -calregulin antibodies were hybridized at the same time to detect potential cross-contamination of the fractions. Fold changes in three independent experiments are shown in the histograms as mean (± S.D.) values. *P < 0.05. n.s., not significant. B. BxPC-3 and L3.6pl cells were treated with gemcitabine (BxPC-3, 200 nM; L3.6pl, 120

nM), cisplatin (BxPC-3, 2.5 μM; L3.6pl, 2 μM), or doxorubicin (BxPC-3, 600 nM; L3.6pl, 400 nM) for 6 h or different concentrations of H_2O_2 for 25 min. Cells were lysed and subjected to Western blotting with the indicated antibodies. GAPDH was used as a loading control.

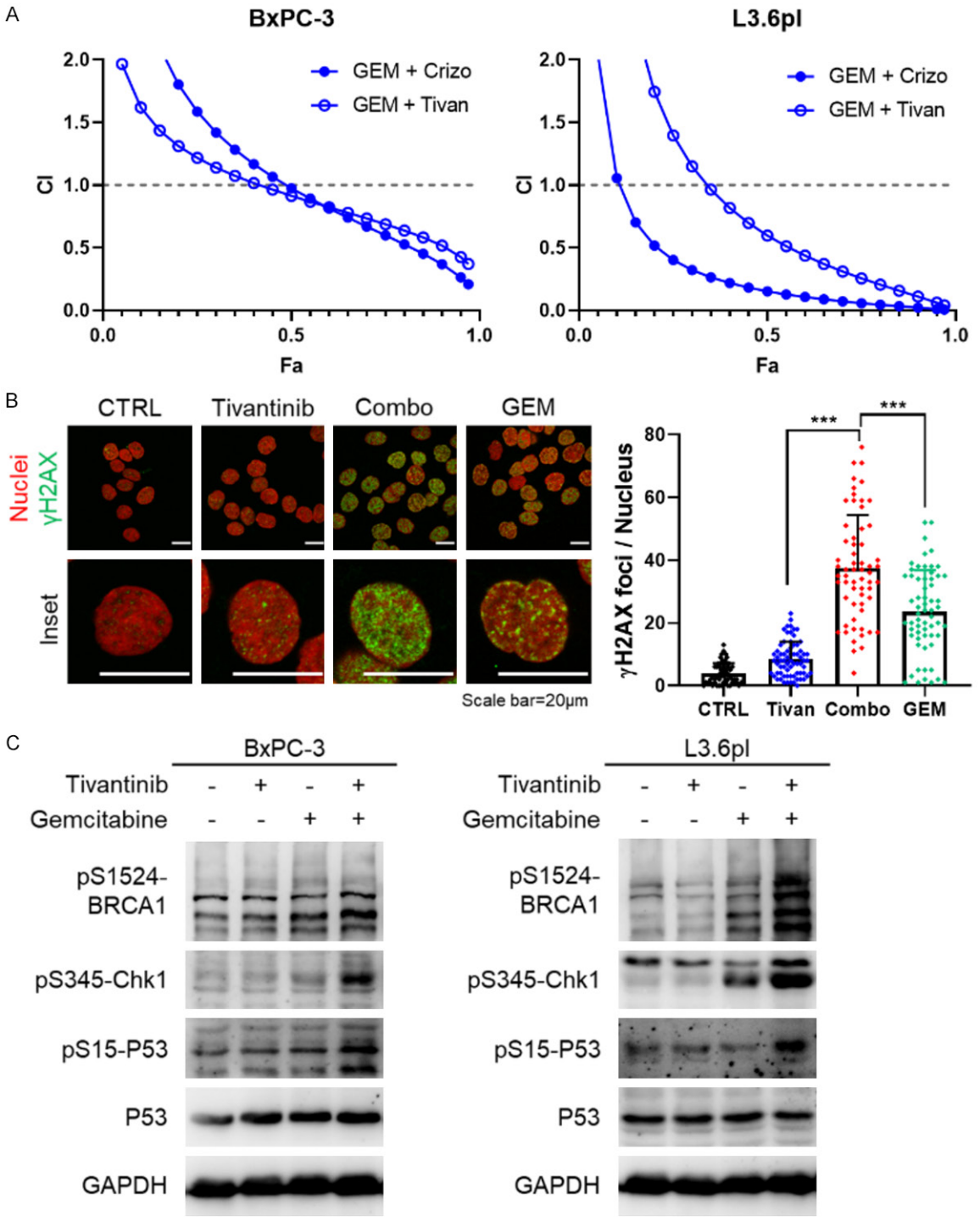

Figure 3. Targeting c-MET with tivantinib and crizotinib sensitizes pancreatic cancer cells to treatment with gemcitabine. A. The synergistic effects of gemcitabine (GEM) and c-MET inhibitors in BxPC-3 and L3.6pl cells as measured using a cell viability assay after 96 h of treatment with them. Crizo, crizotinib; Tivan, tivantinib. B. BxPC-3 cells were treated with tivantinib (0.4 μM), gemcitabine (16 nM), or a combination of the two (Combo) for 16 h before immunofluorescent staining. Representative images of γH2AX (green fluorescence) and DNA (pseudocolored red)

in the cells are shown. Scale bars, 20 μm. The histogram shows mean (± S.D.) values (n > 80). CTRL, control. ***P < 0.001. C. BxPC-3 and L3.6pl cells were treated with gemcitabine (BxPC-3, 16 nM; L3.6pl, 8 nM), tivantinib (0.4 μM), or a combination of the two for 16 h. Next, cells were lysed and subjected to Western blotting with the indicated antibodies. GAPDH was used as a loading control.

on identifying an assessable combination therapy for pancreatic cancer by determining whether strategies proposed for breast cancer treatment can also benefit pancreatic cancer patients. Herein, we demonstrated for the first time that the chemotherapeutic drugs gemcitabine and doxorubicin, serving as ROS-induced cellular stress, promote nuclear localization of c-MET, which results in the resistance of pancreatic cancer cells to chemotherapy as well as PARP inhibitor-based therapy. We further proposed new therapeutic strategies combining c-MET inhibitors and a PARP inhibitor or gemcitabine for advanced pancreatic cancer.

With rapid progress in the development of a novel targeted therapy for cancer, improvements in PDAC treatment have lagged behind the advances made for other malignancies. The 5-year overall survival rate in PDAC patients worldwide only improved from 2.5% in 1970-1977 to 8% in 2007-2013 (https://ourworldindata.org/cancer), and the 5-year relative survival rate was only 10% in the United States in 2010-2016 (www.seer.cancer.gov). For the majority of PDAC patients, cytotoxic chemotherapy remains the standard of care. However, in patients with advanced pancreatic cancer, combinations of cytotoxic therapeutic agents, such as combining nab-paclitaxel and gemcitabine treatment, only provide subtle improvements in overall survival time, usually from weeks to months [30]. Although numerous targeted agents have emerged for pancreatic cancer treatment, such as erlotinib [31] and bevacizumab [32], most of them have been less effective than expected, possibly because of the disease's heterogeneity and a lack of appropriate biomarkers for PDAC. We previously reported that c-MET can translocate into the nucleus and phosphorylate PARP1 at Tyr907 under ROS stimulation to promote DNA repair, resulting in the resistance of triple-negative breast cancer to treatment with a PARP inhibitor [20, 21]. However, whether ROS can stimulate nuclear c-MET translocation and whether the same PARP inhibitor-resistant mechanism applies to pancreatic cancer are unknown. By expanding our findings regarding breast cancer to PDAC, we found that ROS inducing chemotherapeutic agents can induce nuclear accumulation of c-MET and that the PARP1 Tyr907 site is phosphorylated in PDAC cells in response to treatment with H_2O_2.

Researchers observed that the c-MET receptor and its ligand hepatocyte growth factor are upregulated in PDACs [33]. Upregulation of c-MET occurs in the early stages of PDAC development [34]. Recently, researchers examined multiple hepatocyte growth factor/c-Met inhibitors in early-phase clinical trials, demonstrating minimal benefits in PDAC patients [5]. In the present study, we found that the chemotherapeutic drugs gemcitabine and doxorubicin enhanced the nuclear accumulation of c-MET. Combination treatment with c-MET inhibitors and a PARP inhibitor effectively reduced the colony formation of tumor cells while increasing the incidence of DNA breaks, demonstrating that this combination led to an imbalance in DNA damage and repair in PDAC cells. Our findings suggest that our study is a promising step in broadening the spectrum of targeted therapy in PDAC patients. For PDAC patients carrying tumors with high c-MET activity levels, combination treatment with a c-MET inhibitor and gemcitabine may produce an antitumor effect with a lower dose of gemcitabine than a single agent strategy, which may alleviate the side effects of cytotoxic chemotherapy. A previous study showed that crizotinib, one of the pan-kinase inhibitors that can target c-MET, increases the blood concentration of gemcitabine, improving the antitumor effect of this drug [35]. Our findings provide additional mechanisms underlying the synergy of crizotinib and gemcitabine and strengthen the rational basis for combining a c-MET inhibitor with first-line ROS-generating chemotherapeutic agents such as gemcitabine and doxorubicin. However, because we found that treatment with cisplatin cannot induce nuclear accumulation of c-MET, further studies are needed to determine whether the combination of a c-MET inhibitor and cisplatin can provide a therapeutic benefit similar to that of the combination of a c-MET inhibitor and gemcitabine in PDAC patients.

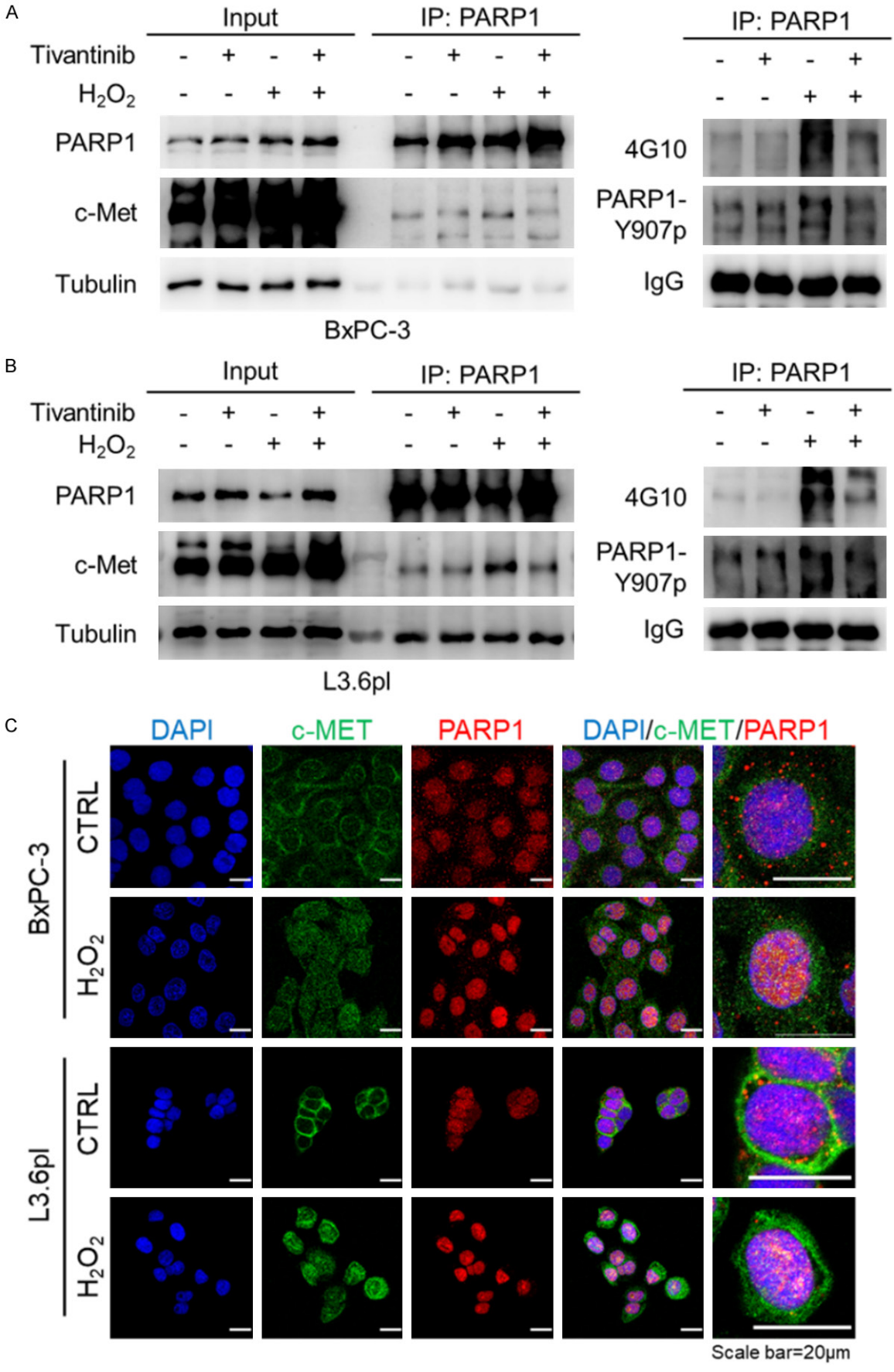
A
Input
IP: PARP1
IP: PARP1
Tivantinib
H2O2
PARP1
c-Met
Tubulin
4G10
PARP1-Y907p
IgG
BxPC-3
B
Input
IP: PARP1
IP: PARP1
Tivantinib
H2O2
PARP1
c-Met
Tubulin
4G10
PARP1-Y907p
IgG
L3.6pl
C
DAPI
c-MET
PARP1
DAPI/c-MET/PARP1
BxPC-3
CTRL
H2O2
L3.6pl
CTRL
H2O2
Scale bar=20μm

Figure 4. c-MET interacts with PARP1 and phosphorylates it at Tyr907. (A and B) BxPC-3 (A) and L3.6pl (B) cells were treated with 5 mM H_2O_2 for 30 min in the presence or absence of the c-MET inhibitor tivantinib (2 μM, pretreated for 4 h). The cells were then subjected to co-immunoprecipitation (IP) with an anti-PARP antibody followed by Western blotting with the indicated antibodies. Tubulin and IgG were used as controls. (C) BxPC-3 and L3.6pl cells were treated with 5 mM H_2O_2 for 30 min before being fixed, permeabilized, and blocked. The cells were then incubated with anti-DAPI (blue fluorescence), anti-c-MET (green fluorescence), and anti-PARP1 (red fluorescence) antibodies. Insets, enlarged views of the interaction between c-MET and PARP1. Scale bars, 20 μm. CTRL, control.

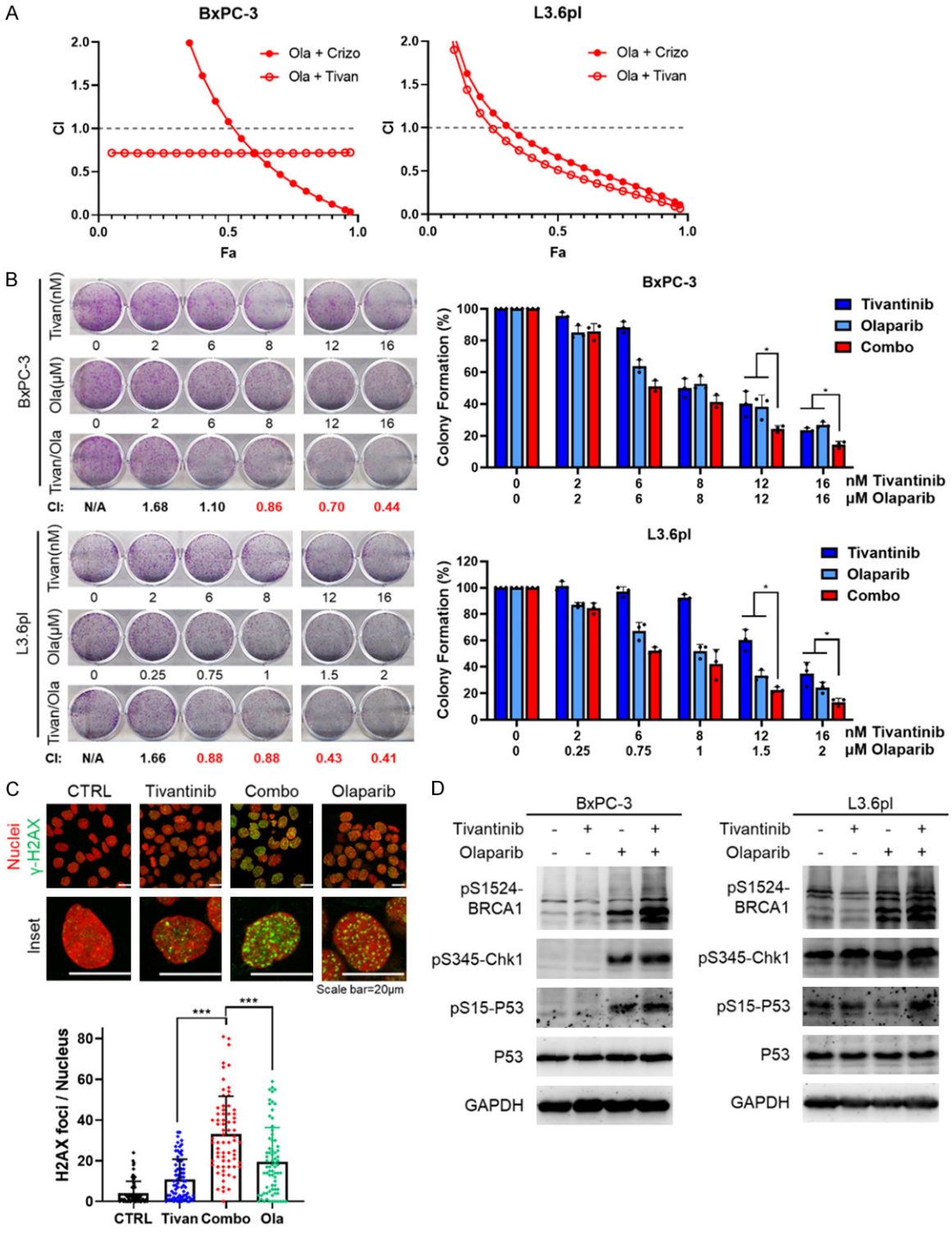

Figure 5. Potential therapeutic strategy targeting c-MET and PARP in pancreatic cancer cells. A. The synergistic effects of the PARP inhibitor olaparib (Ola) and c-MET inhibitors in BxPC-3 and L3.6pl cells were measured using a cell viability assay after 96 h of treatment. Crizo, crizotinib; Tivan, tivantinib. B. BxPC-3 and L3.6pl cells were treated with tivantinib, olaparib, or both at the indicated concentrations for 10-14 days. The cells were then fixed and stained for colony formation assay. The number of colonies formed was normalized according to that in the control group (no treatment). Mean (± S.D.) values from three independent experiments are shown in the histogram. $*P < 0.05$. C. BxPC-3 cells were treated with tivantinib (0.4 μM), olaparib (120 μM), or both (Combo) for 16 h before immunofluorescent staining. Representative images of γH2AX (green fluorescence) and DNA (pseudocolored red) in the cells are shown. Scale bars, 20 μm. The histogram shows mean (± S.D.) values (n > 80). $***P < 0.001$. D. BxPC-3 and L3.6pl cells were treated with olaparib (BxPC-3, 60 μM; L3.6pl, 8 μM) and tivantinib (0.4 μM) either alone or combined for 16 h. The cells were then lysed and hybridized with the indicated antibodies in Western blotting. GAPDH was used in Western blotting as a loading control.

Investigators have evaluated PARP inhibitors in pancreatic cancer clinical trials [36], and our previous study found that nuclear c-MET contributes to PARP inhibitor resistance in breast cancer cells [21]. In the present study, we demonstrated that nuclear c-MET interacted with and phosphorylated PARP1 in response to ROS stimulation in PDAC cells. This phenomenon is similar to our previous findings of breast cancer studies [20, 21]. Therefore, our findings reported herein suggest that nuclear c-MET also contributes to the PARP inhibitor resistance of pancreatic cancer. Indeed, by treating PDAC cells with olaparib combined with either tivantinib or crizotinib, we demonstrated that the combination of a PARP inhibitor and a c-MET inhibitor has a synergistic effect in eliminating PDAC cells by increasing DNA damage in them. Further mechanistic research and efficacy evaluations involving patient-derived preclinical models are important for guiding the development of this new therapeutic approach and understanding biological and clinical responses of PDAC to it. The present study implies that a combination treatment with a c-MET inhibitor and PARP inhibitor will benefit PDAC patients regardless of their BRCA mutation status. Our findings also may contribute to broadening the therapeutic applications of PARP inhibitors in the future.

In summary, our data suggest that the use of chemotherapy promotes the nuclear localization of c-MET in tumor cells, resulting in resistance to PARP inhibitor-based therapy and chemotherapy. We propose new therapeutic strategies combining c-MET inhibitors and a PARP inhibitor or gemcitabine for advanced pancreatic cancer.

Acknowledgements

We thank Mr. Donald Norwood in Editing Services, Research Medical Library at The University of Texas MD Anderson Cancer Center for detailed editing of this manuscript. Sanger DNA sequencing was supported by the NIH/NCI under award number P30CA016672 and used the Advanced Technology Genomics Core at MD Anderson. This work was funded in part by NCI grant 5R01CA211615-02, the MD Anderson-China Medical University Sister Institution Fund, China Scholarship Council Program grant 201806230249 (to Y.G.), and T32 Training Grant in Cancer Biology 5T32CA186892 (to M.-K.C.).

Disclosure of conflict of interest

None.

Address correspondence to: Mien-Chie Hung, Office of The President, China Medical University, 91 Hsueh-Shih Road, North District, Taichung 40402, Taiwan. Tel: +886-422053366; Fax: +886-42206-0248; E-mail: mhung@cmu.edu.tw; mhung77030@gmail.com; Mei-Kuang Chen, Department of Molecular and Cellular Oncology, The University of Texas MD Anderson Cancer Center, 1515 Holcombe Boulevard, Houston 77030, TX, USA. Tel: +832-750-6641; E-mail: mchen6@mdanderson.org; Yingbin Liu, Department of Biliary-Pancreatic Surgery, Renji Hospital, School of Medicine, Shanghai Jiao Tong University, 160 Pujian Road, Shanghai 200127, China. Tel: +86-21-68382510; E-mail: laoniulyb@shsmu.edu.cn

References

[1] McGuigan A, Kelly P, Turkington RC, Jones C, Coleman HG and McCain RS. Pancreatic cancer: a review of clinical diagnosis, epidemiology, treatment and outcomes. World J Gastroenterol 2018; 24: 4846-4861.

[2] Siegel RL, Miller KD and Jemal A. Cancer statistics, 2020. CA Cancer J Clin 2020; 70: 7-30.

[3] Pour PM, Bell RH and Batra SK. Neural invasion in the staging of pancreatic cancer. Pancreas 2003; 26: 322-325.

[4] de Sousa Cavalcante L and Monteiro G. Gemcitabine: metabolism and molecular mechanisms of action, sensitivity and chemoresistance in pancreatic cancer. Eur J Pharmacol 2014; 741: 8-16.
[5] Yap TA, Olmos D, Brunetto AT, Tunariu N, Barriuso J, Riisnaes R, Pope L, Clark J, Futreal A, Germuska M, Collins D, deSouza NM, Leach MO, Savage RE, Waghorne C, Chai F, Garmey E, Schwartz B, Kaye SB and de Bono JS. Phase I trial of a selective c-MET inhibitor ARQ 197 incorporating proof of mechanism pharmacodynamic studies. J Clin Oncol 2011; 29: 1271-1279.
[6] Rosen LS, Senzer N, Mekhail T, Ganapathi R, Chai F, Savage RE, Waghorne C, Abbadessa G, Schwartz B and Dreicer R. A phase I dose-escalation study of Tivantinib (ARQ 197) in adult patients with metastatic solid tumors. Clin Cancer Res 2011; 17: 7754-7764.
[7] Schöffski P, Sgroi M, Burris HA, Lutzky J, Rearden T, Sikic B, Stephenson J, Elhardt D, Lee Y and Kurzrock R. 371 Phase 2 randomized discontinuation trial (RDT) of XL184 in patients (pts) with advanced solid tumors. EJC Suppl 2010; 8: 117.
[8] Sharma N and Adjei AA. In the clinic: ongoing clinical trials evaluating c-MET-inhibiting drugs. Ther Adv Med Oncol 2011; 3: S37-50.
[9] Maitra A and Hruban RH. Pancreatic cancer. Annu Rev Pathol 2008; 3: 157-188.
[10] Koong AC, Mehta VK, Le QT, Fisher GA, Terris DJ, Brown JM, Bastidas AJ and Vierra M. Pancreatic tumors show high levels of hypoxia. Int J Radiat Oncol Biol Phys 2000; 48: 919-22.
[11] Gorrini C, Harris IS and Mak TW. Modulation of oxidative stress as an anticancer strategy. Nat Rev Drug Discov 2013; 12: 931-947.
[12] Zhang Z, Duan Q, Zhao H, Liu T, Wu H, Shen Q, Wang C and Yin T. Gemcitabine treatment promotes pancreatic cancer stemness through the Nox/ROS/NF-kappaB/STAT3 signaling cascade. Cancer Lett 2016; 382: 53-63.
[13] Arora S, Bhardwaj A, Singh S, Srivastava SK, McClellan S, Nirodi CS, Piazza GA, Grizzle WE, Owen LB and Singh AP. An undesired effect of chemotherapy: gemcitabine promotes pancreatic cancer cell invasiveness through reactive oxygen species-dependent, nuclear factor kappaB- and hypoxia-inducible factor 1alpha-mediated up-regulation of CXCR4. J Biol Chem 2013; 288: 21197-21207.
[14] Sugimura K, Takebayashi S, Taguchi H, Takeda S and Okumura K. PARP-1 ensures regulation of replication fork progression by homologous recombination on damaged DNA. J Cell Biol 2008; 183: 1203-1212.
[15] Liu Q, Gheorghiu L, Drumm M, Clayman R, Eidelman A, Wszolek MF, Olumi A, Feldman A, Wang M, Marcar L, Citrin DE, Wu CL, Benes CH, Efstathiou JA and Willers H. PARP-1 inhibition with or without ionizing radiation confers reactive oxygen species-mediated cytotoxicity preferentially to cancer cells with mutant TP53. Oncogene 2018; 37: 2793-2805.
[16] Hou D, Liu Z, Xu X, Liu Q, Zhang X, Kong B, Wei JJ, Gong Y and Shao C. Increased oxidative stress mediates the antitumor effect of PARP inhibition in ovarian cancer. Redox Biol 2018; 17: 99-111.
[17] Slade D. PARP and PARG inhibitors in cancer treatment. Genes Dev 2020; 34: 360-394.
[18] Golan T, Hammel P, Reni M, Van Cutsem E, Macarulla T, Hall MJ, Park JO, Hochhauser D, Arnold D, Oh DY, Reinacher-Schick A, Tortora G, Algul H, O'Reilly EM, McGuinness D, Cui KY, Schlienger K, Locker GY and Kindler HL. Maintenance olaparib for germline BRCA-mutated metastatic pancreatic cancer. N Engl J Med 2019; 381: 317-327.
[19] Blair AB, Groot VP, Gemenetzis G, Wei J, Cameron JL, Weiss MJ, Goggins M, Wolfgang CL, Yu J and He J. BRCA1/BRCA2 germline mutation carriers and sporadic pancreatic ductal adenocarcinoma. J Am Coll Surg 2018; 226: 630-637, e631.
[20] Chen MK, Du Y, Sun L, Hsu JL, Wang YH, Gao Y, Huang J and Hung MC. H2O2 induces nuclear transport of the receptor tyrosine kinase c-MET in breast cancer cells via a membrane-bound retrograde trafficking mechanism. J Biol Chem 2019; 294: 8516-8528.
[21] Du Y, Yamaguchi H, Wei Y, Hsu JL, Wang HL, Hsu YH, Lin WC, Yu WH, Leonard PG, Lee GRt, Chen MK, Nakai K, Hsu MC, Chen CT, Sun Y, Wu Y, Chang WC, Huang WC, Liu CL, Chang YC, Chen CH, Park M, Jones P, Hortobagyi GN and Hung MC. Blocking c-Met-mediated PARP1 phosphorylation enhances anti-tumor effects of PARP inhibitors. Nat Med 2016; 22: 194-201.
[22] Han Y, Chen MK, Wang HL, Hsu JL, Li CW, Chu YY, Liu CX, Nie L, Chan LC, Yam C, Wang SC, He GJ, Hortobagyi GN, Tan XD and Hung MC. Synergism of PARP inhibitor fluzoparib (HS10160) and MET inhibitor HS10241 in breast and ovarian cancer cells. Am J Cancer Res 2019; 9: 608-618.
[23] Dong Q, Du Y, Li H, Liu C, Wei Y, Chen MK, Zhao X, Chu YY, Qiu Y, Qin L, Yamaguchi H and Hung MC. EGFR and c-MET cooperate to enhance resistance to PARP inhibitors in hepatocellular carcinoma. Cancer Res 2019; 79: 819-829.
[24] Chu YY, Yam C, Chen MK, Chan LC, Xiao M, Wei YK, Yamaguchi H, Lee PC, Han Y, Nie L, Sun X, Moulder SL, Hess KR, Wang B, Hsu JL, Hortobagyi GN, Litton J, Chang JT and Hung MC. Blocking c-Met and EGFR reverses ac-

quired resistance of PARP inhibitors in triple-negative breast cancer. Am J Cancer Res 2020; 10: 648-661.
[25] Chen MK, Hsu JL and Hung MC. Nuclear receptor tyrosine kinase transport and functions in cancer. Adv Cancer Res 2020; 147: 59-107.
[26] Chou TC. Theoretical basis, experimental design, and computerized simulation of synergism and antagonism in drug combination studies. Pharmacol Rev 2006; 58: 621-681.
[27] Munshi N, Jeay S, Li Y, Chen CR, France DS, Ashwell MA, Hill J, Moussa MM, Leggett DS and Li CJ. ARQ 197, a novel and selective inhibitor of the human c-Met receptor tyrosine kinase with antitumor activity. Mol Cancer Ther 2010; 9: 1544-1553.
[28] Christensen JG, Zou HY, Arango ME, Li Q, Lee JH, McDonnell SR, Yamazaki S, Alton GR, Mroczkowski B and Los G. Cytoreductive antitumor activity of PF-2341066, a novel inhibitor of anaplastic lymphoma kinase and c-Met, in experimental models of anaplastic large-cell lymphoma. Mol Cancer Ther 2007; 6: 3314-3322.
[29] Zhao H, Wu S, Li H, Duan Q, Zhang Z, Shen Q, Wang C and Yin T. ROS/KRAS/AMPK signaling contributes to gemcitabine-induced stem-like cell properties in pancreatic cancer. Mol Ther Oncolytics 2019; 14: 299-312.
[30] Von Hoff DD, Ervin T, Arena FP, Chiorean EG, Infante J, Moore M, Seay T, Tjulandin SA, Ma WW, Saleh MN, Harris M, Reni M, Dowden S, Laheru D, Bahary N, Ramanathan RK, Tabernero J, Hidalgo M, Goldstein D, Van Cutsem E, Wei X, Iglesias J and Renschler MF. Increased survival in pancreatic cancer with nab-paclitaxel plus gemcitabine. N Engl J Med 2013; 369: 1691-1703.
[31] Moore MJ, Goldstein D, Hamm J, Figer A, Hecht JR, Gallinger S, Au HJ, Murawa P, Walde D, Wolff RA, Campos D, Lim R, Ding K, Clark G, Voskoglou-Nomikos T, Ptasynski M and Parulekar W; National Cancer Institute of Canada Clinical Trials Group. Erlotinib plus gemcitabine compared with gemcitabine alone in patients with advanced pancreatic cancer: a phase III trial of the national cancer institute of canada clinical trials group. J Clin Oncol 2007; 25: 1960-1966.
[32] Van Cutsem E, Vervenne WL, Bennouna J, Humblet Y, Gill S, Van Laethem JL, Verslype C, Scheithauer W, Shang A, Cosaert J and Moore MJ. Phase III trial of bevacizumab in combination with gemcitabine and erlotinib in patients with metastatic pancreatic cancer. J Clin Oncol 2009; 27: 2231-2237.
[33] Jones S, Zhang X, Parsons DW, Lin JC, Leary RJ, Angenendt P, Mankoo P, Carter H, Kamiyama H, Jimeno A, Hong SM, Fu B, Lin MT, Calhoun ES, Kamiyama M, Walter K, Nikolskaya T, Nikolsky Y, Hartigan J, Smith DR, Hidalgo M, Leach SD, Klein AP, Jaffee EM, Goggins M, Maitra A, Iacobuzio-Donahue C, Eshleman JR, Kern SE, Hruban RH, Karchin R, Papadopoulos N, Parmigiani G, Vogelstein B, Velculescu VE and Kinzler KW. Core signaling pathways in human pancreatic cancers revealed by global genomic analyses. Science 2008; 321: 1801-1806.
[34] Yu J, Ohuchida K, Mizumoto K, Ishikawa N, Ogura Y, Yamada D, Egami T, Fujita H, Ohashi S, Nagai E and Tanaka M. Overexpression of c-met in the early stage of pancreatic carcinogenesis; altered expression is not sufficient for progression from chronic pancreatitis to pancreatic cancer. World J Gastroenterol 2006; 12: 3878-3882.
[35] Avan A, Caretti V, Funel N, Galvani E, Maftouh M, Honeywell RJ, Lagerweij T, Van Tellingen O, Campani D, Fuchs D, Verheul HM, Schuurhuis GJ, Boggi U, Peters GJ, Wurdinger T and Giovannetti E. Crizotinib inhibits metabolic inactivation of gemcitabine in c-Met-driven pancreatic carcinoma. Cancer Res 2013; 73: 6745-6756.
[36] Patel R, Fein D, Ramirez CB, Do K and Saif MW. PARP inhibitors in pancreatic cancer: from phase i to plenary session. Pancreas (Fairfax) 2019; 3: e5-e8.